Title

Reorganization of the functional connectome from rest to a visual perception task in schizophrenia and bipolar disorder.

Permalink

Authors

Riedel, Philipp

Lee, Junghee

Watson, Christopher

et al.

Publication Date

DOI

Peer reviewed

Reorganization of the Functional Connectome from Rest to a Visual Perception Task in Schizophrenia and Bipolar Disorder

Philipp Riedel[a,b,*], **Junghee Lee**[a,c,d], **Christopher G. Watson**[e], **Amy M. Jimenez**[c,a], **Eric A. Reavis**[a,c], **Michael F. Green**[c,a]

[a]Semel Institute for Neuroscience and Human Behavior, University of California Los Angeles, Los Angeles, 760 Westwood Plaza, Los Angeles, CA 90024; USA

[b]Department of Psychiatry and Neuroimaging Center, Technische Universität Dresden, Würzburger Straße 35, 01187 Dresden; Germany

[c]Desert Pacific Mental Illness Research, Education, and Clinical Center, Greater Los Angeles VA Healthcare System, Bldg. 210, 11301 Wilshire Blvd, Los Angeles, CA 90073; USA

[d]Department of Psychiatry and Behavioral Neurobiology, School of Medicine, The University of Alabama at Birmingham, SC 560, 1720 2nd Ave S, Birmingham, AL 35294-0017; USA

[e]Department of Physical Medicine and Rehabilitation, Baylor College of Medicine, One Baylor Plaza, Houston, TX 77030; USA

Abstract

Functional connectome organization is altered in schizophrenia (SZ) and bipolar disorder (BD). However, it remains unclear whether network *reorganization* during a task relative to rest is also altered in these disorders.

This study examined connectome organization in patients with SZ (N=43) and BD (N=42) versus healthy controls (HC; N=39) using fMRI data during a visual object-perception task and at rest. Graph analyses were conducted for the whole-brain network using indices selected a priori: three reflecting network segregation (clustering coefficient, local efficiency, modularity), two reflecting integration (characteristic path length, global efficiency).

Group differences were limited to network segregation and were more evident in SZ (clustering coefficient, modularity) than in BD (clustering coefficient) compared to HC. State differences

[*]Corresponding Author: PR, riedel.philipp@posteo.de, 0049-351-458-2797.

were found across groups for segregation (local efficiency) and integration (characteristic path length). There was no group-by-state interaction for any graph index.

In summary, aberrant network organization compared to HC was confirmed, and was more evident in SZ than in BD. Yet, reorganization was largely intact in both disorders. These findings help to constrain models of dysconnection in SZ and BD, suggesting that the extent of functional dysconnectivity in these disorders tends to persist across changes in mental state.

Keywords

dysconnection; graph analysis; integration; resting-state connectivity; segregation; task-based connectivity

1 Introduction

Theories of brain dysconnectivity in schizophrenia (SZ) and bipolar disorder (BD) are widely held (Friston, Brown, Siemerkus, & Stephan, 2016; Friston & Frith, 1995; Khadka et al., 2013; Perry, Roberts, Mitchell, & Breakspear, 2018; Pettersson-Yeo, Allen, Benetti, McGuire, & Mechelli, 2011; Stephan, Friston, & Frith, 2009; Van Den Heuvel & Fornito, 2014). Consistent with these theories, there is good evidence of aberrant functional connectivity in SZ and BD (Cao, Dixson, Meyer-Lindenberg, & Tost, 2016; Gong et al., 2021), including findings showing an aberrant organization of the functional connectome (i.e., the entire network of all functional connections in the brain) (Kambeitz et al., 2016; Narr & Leaver, 2015; Perry et al., 2018). Yet, functional connectome organization is not static across states. In healthy participants, *reorganization* occurs, for example, during a task compared to rest (Bolt, Nomi, Rubinov, & Uddin, 2017). It remains unclear, whether functional connectome *reorganization* is also aberrant in SZ and BD compared to HC. This knowledge would inform current theories of dysconnectivity in these disorders.

Using graph theory (Rubinov & Sporns, 2010), functional connectome organization can be characterized according to two principles of network organization: segregation and integration. *Segregation* describes the extent to which a network exhibits a functional clustering of regions (i.e., nodes) for specialized, modular processing. *Integration* describes the efficiency of information transfer across the whole network. Past research revealed abnormalities in both segregation and integration of the functional connectome in SZ and BD, primarily using resting-state data (Kambeitz et al., 2016; Lei et al., 2019; Perry et al., 2018; Wang et al., 2017; Z. Yu et al., 2020). Three indices of segregation have emerged as particularly aberrant in these disorders: the clustering coefficient (C_p), local efficiency (E_{loc}), and modularity (Q) (Alexander-Bloch et al., 2012; He et al., 2012; Lynall et al., 2010). C_p refers to the 'clustering' of nodes and is the average probability that two nodes connected to a given node will also be connected to one another. E_{loc} reflects the capacity for information transfer between adjacent nodes when a given node of interest is removed. While C_p and E_{loc} emphasize the topology of adjacent nodes across the network, Q measures 'clustering' of a large number of nodes and therefore describes how well the network can be partitioned into modules (e.g., into different cognitive control networks) (see also Methods: 2.6.3). With few exceptions (Hadley et al., 2016; Q. Yu et al., 2011), most graph analyses in SZ show

a lower degree of functional network segregation as indicated by a decrease in C_p (He et al., 2012; Liu et al., 2008; Lynall et al., 2010; S. Ma, Calhoun, Eichele, Du, & Adali, 2012; Xia et al., 2019), E_{loc}, and Q (Alexander-Bloch et al., 2010, 2012; He et al., 2012; Q. Ma et al., 2020). With respect to integration, two indices in particular were examined in SZ and BD: the characteristic path length (L_p) and global efficiency (E_{glob}). L_p describes how directly all pairs of nodes in the network are connected. E_{glob} describes the capacity for parallel exchange of information within the whole network. Findings on L_p and E_{glob} for both disorders, though, have been somewhat mixed (Doucet, Bassett, Yao, Glahn, & Frangou, 2017; Kambeitz et al., 2016; Wang et al., 2017; Xia et al., 2019). Above findings on altered functional connectome organization in SZ and BD are consistent with and further support a pathophysiological theory of dysconnectivity in these disorders, but are limited to *either* the resting *or* task state.

However, functional connectome organization is not static (Calhoun, Kiehl, & Pearlson, 2008; Cole, Bassett, Power, Braver, & Petersen, 2014; Finc et al., 2020; P. Jiang et al., 2018; T. Jiang, He, Zang, & Weng, 2004; Kieliba, Madugula, Filippini, Duff, & Makin, 2019). For example, in healthy participants, network segregation and integration are increased during a task compared to rest (Bolt et al., 2017), which is particularly evident in the visual domain (Breckel et al., 2013; Ulloa & Horwitz, 2018). Interestingly, impaired visual perception is prevalent in SZ and BD (Butler, Silverstein, & Dakin, 2008; Javitt & Freedman, 2016; Rassovsky, Horan, Lee, Sergi, & Green, 2011). To date, however, no study has examined the reorganization of the functional connectome from rest to a visual task in SZ and BD. A few studies investigating connectome segregation and integration in a task and at rest were limited to an auditory task and did not include BD (S. Ma et al., 2012; Q. Yu, Sui, Kiehl, Pearlson, & Calhoun, 2013).

Thus, in this study, we conducted a secondary analysis using a unique fMRI dataset on visual processing in SZ and BD. Resting-state data and data from a visual object recognition task were acquired in the same session for each of the SZ (N=43), BD (N=42), and HC (N=39) participants (Jimenez, Riedel, Lee, Reavis, & Green, 2019; Reavis et al., 2020; Reavis, Lee, Wynn, Narr, et al., 2017). Whole-brain functional connectome reorganization between task performance and rest was examined using established indices of network segregation and integration from graph theory mentioned above. Modularity (Q) in particular was explored in more detail using two types of nodes: 'provincial hubs', which are important for within-module communication (i.e., segregation), and 'connector hubs', which are important for between-module integration.

Consistent with existing data on brain dysconnectivity in SZ and BD, we hypothesized a lower degree of functional network segregation (C_p, E_{loc}, Q) and largely intact network integration (L_p, E_{glob}) in both disorders. Specific hypotheses regarding the rest-to-task reorganization of the functional connectome in SZ and BD compared to HC could not be made because of a lack of consistent and comparable prior data (S. Ma et al., 2012; Q. Yu et al., 2013). However, we anticipated a number of possible patterns of functional connectome reorganization in patients, each of which would extend theories of brain dysconnectivity in SZ and BD. First, network reorganization may be similar in magnitude in these disorders compared to HC, which would indicate that adjustment to cognitive demands is not aberrant.

This pattern seemed less likely given the robust previous findings of dysorganization of the functional connectome in SZ and BD (Narr & Leaver, 2015; Perry et al., 2018), which have emerged to some degree in task-related, but most notably in resting-state fMRI studies (Kambeitz et al., 2016). If, on the other hand, reorganization is greater in SZ and BD than in HC, such that dysorganization proves less pronounced during a task compared to rest, this would indicate a compensatory mechanism in adapting to cognitive demands. Conversely, if reorganization is lower in SZ and BD than in HC, this would indicate impaired reorganization in addition to marked resting-state dysconnectivity. This last pattern is most readily inferred from what we currently know about brain dysconnectivity in SZ and BD.

2 Methods

The study protocol was reviewed and approved by the Institutional Review Boards of the VA Greater Los Angeles Healthcare System (GLA) and the University of California, Los Angeles (UCLA).

2.1 Participants

A total of 49 individuals with SZ, 49 individuals with BD, and 52 HC completed both task and resting-state fMRI as part of a large, NIMH-sponsored study of visual processing in major mental illness. Every individual had the capacity to give informed consent and provided written informed consent prior to participation. All patient participants were clinically stable outpatients with a DSM-IV diagnosis of SZ or BD (First, Gibbon, Spitzer, Williams, & Benjamin, 1997). For detailed selection criteria please refer to the supplement (1.1).

Clinical symptoms were characterized for the patient participants using the Brief Psychiatric Rating Scale (BPRS) (Ventura, Nuechterlein, Subotnik, & Gilbert, 1995), Clinical Assessment Interview for Negative Symptoms (CAINS) (Kring, Gur, Blanchard, Horan, & Reise, 2013), Young Mania Rating Scale (YMRS) (Young, Biggs, Ziegler, & Meyer, 1978), and Hamilton Depression rating scale (HAMD) (Hamilton, 1960). Mean daily doses for antipsychotic medication were calculated in chlorpromazine equivalents (Andreasen, Pressler, Nopoulos, Miller, & Ho, 2010) for each patient, based on available self-report.

2.2 Visual Perception Task

A visual object-perception task (Reavis, Lee, Wynn, Engel, et al., 2017) was used for task-based fMRI (Fig. 1). In the task, participants viewed five images: two different chairs, two different cups, and one outdoor scene. Two object-stimulus blocks for each of the five images and two blocks containing only a fixation cross were presented in a shuffled order in each of the five task runs (i.e., 50 object-stimulus blocks total, 10 fixation-cross blocks total). In each object-stimulus block, the image flashed on for 1000 ms and off for 400 ms ten times, appearing in slightly different locations each time (i.e., 500 visual stimuli total). In about 20% of the presentations, the image was missing a part (e.g., a cup missing a handle) (i.e., ~ 100 target stimuli total). Subjects were asked to press a button each time they detected a missing part. The percentage of correct responses to these presentations was

recorded across all five task runs as a behavioural marker of ongoing vigilance (see Table 1). Thus, the task required ongoing vigilance, but was designed to place relatively little demand on memory or cognitive control to help reduce differences in performance between patients and controls. Performance differences could confound group comparisons of connectome reorganization between resting-state and task-based fMRI. Only the first two task runs were used for fMRI data processing (see 2.5).

2.3 fMRI acquisition

Scanning was performed on a Siemens Tim Trio 3 T MRI scanner equipped with a 12-channel head coil (Siemens Medical Solutions, Erlangen, Germany) at the UCLA Staglin Center for Cognitive Neuroscience. Five task fMRI runs (200 s each) and one resting-state fMRI run (300 s) were acquired using matched and standard parameters (see supplement: 1.2). After the final task run, a retinotopic mapping scan (about 2.5 min) and a diffusion-weighted imaging scan (about 9 min) (both of which are not part of this study) were acquired before the resting-state scan. Because the acquisition parameters were tailored for the examination of visual processing (see 1), the fMRI field of view was not optimized to cover the whole brain in all participants (see 2.5 and supplement: 1.4.2).

2.4 Motion assessment

Framewise displacement (FD) (Power, Barnes, Snyder, Schlaggar, & Petersen, 2012) was calculated to quantify motion between fMRI volumes. A threshold of relative FD > 0.5 mm (as suggested by Power et al., 2014) was used to tag outlier volumes for later nuisance regression / scrubbing. Additional parameters were used to exclude participants with excessive motion and to assess potentially confounding effects of motion (see supplement: 1.3).

2.5 fMRI data processing

fMRI data processing was performed in FSL version 5.0.9 (Jenkinson, Beckmann, Behrens, Woolrich, & Smith, 2012), as briefly summarized here. See the supplement (1.4) for details. The identical data preprocessing was used for resting-state and task-based fMRI.

First-level analysis was performed in subject-space to avoid both image distortion due to normalization, especially in the clinical groups, and changes in the graph indices due to resampling and interpolation (Fryer et al., 2019; Gargouri et al., 2018; Magalhães, Marques, Soares, Alves, & Sousa, 2015; van de Ven, Rotarska Jagiela, Oertel-Knöchel, & Linden, 2017).

Nuisance regression of six motion parameters, outlier volumes (FD > 0.5 mm, i.e., motion scrubbing), and mean white matter (WM) and cerebrospinal fluid (CSF) signal was performed. Global signal regression was not performed. For the task-based fMRI analyses, deconvolution of the functional data was also performed during first-level analysis, by modelling the response of each voxel to ten object-stimulus blocks (i.e., two blocks for each of the five stimuli) in each of the five task runs. Fixation-cross blocks were not explicitly modelled.

We were primarily interested in reorganization from rest to task. As resting-state and task-based fMRI differ in various ways, we decided to equate the amount of fMRI data from which the graph indices were derived in each state, as has been done in previous studies (Q. Yu et al., 2013). Thus, the first two of the task-based fMRI runs were selected for the current analyses because they were similar in length to the resting state run. Using a larger amount of data from the task might have increased reliability of the graph indices for the task condition, but would have reduced comparability of the indices with the resting-state fMRI run. After scrubbing, there were at least 3.8 min of resting-state fMRI in each participant, and an average of about 4.5 min across the sample. There were at least 5 min of task-based fMRI, and an average of about 6 min.

The mean Blood Oxygen Level Dependent (BOLD) signal time course for all nodes as defined in the Power atlas (Power et al., 2011) was extracted from the residual images for both the task-based and resting-state fMRI data ('res4d.nii.gz'). A narrowed field of view and individual brain anatomy contributed to participants having different sets of covered nodes (see supplement: 1.4.2). However, when the number of nodes varies, the graph indices are difficult to compare between groups (van Wijk, Stam, & Daffertshofer, 2010). Rather than excluding a large number of participants from this unique sample due to incomplete coverage of a few nodes, we decided to prioritize statistical power by focusing on the set of nodes for which there was similar coverage across participants. As a result, 60 of the 264 Power nodes were excluded from the main analyses. A supplemental analysis in a subset of participants with complete coverage of all 264 Power nodes was performed (see supplement: 1.6.5).

2.6   Graph analysis of functional connectivity

2.6.1   Transformation of correlation matrices—Pearson time-series correlation coefficients (r) for all node pairs were calculated to form a 204×204 matrix for each participant, with the diagonal and connections with negative correlation coefficients set to 0. We considered alternative ways to transform negative r values (see supplement: 1.5, 2.3). All participants had a network density greater than 50% for both rest and task. Connectivity matrices were Fisher-z-transformed.

2.6.2   Graph construction—Graph analyses were performed using the R package *brainGraph*, version 2.2.0 (Watson, 2018). For the main analyses, correlation matrices were binarized using a range of density (proportional) thresholds (strongest 10% to 50% of edges in 2% increments; see supplement 1.6.1). Binarization reduces potential effects of global connectivity on the graph indices, as it removes all edge-weight variance. Supplemental analyses were also conducted using raw (absolute) thresholding (supplement: 1.6.1).

2.6.3   Assessment of graph indices—Graph analyses were conducted for the whole-brain network (see supplement: 1.6). Network segregation was assessed using the clustering coefficient (C_p), local efficiency (E_{loc}), and modularity (Q) (Rubinov & Sporns, 2010). C_p refers to the 'clustering' of nodes into groups of three and is the probability that two nodes connected to a given node (i.e., 'adjacent' nodes) will also be connected to one another, averaged over the whole network. E_{loc} relates to adjacent nodes and reflects the

capacity for information transfer between adjacent nodes when a given node of interest is removed. While C_p and E_{loc} emphasize the topology of *adjacent nodes* across the network, Q measures 'clustering' of a *large number of nodes* into larger groups and reflects the connectivity within these groups (i.e., modules) relative to the connectivity between the groups. That is, Q describes how well the brain network can be partitioned into modules (Blondel, Guillaume, Lambiotte, & Lefebvre, 2008; Newman, 2006). Q was computed using the Louvain algorithm (Blondel et al., 2008).

Whole-brain network integration was assessed using characteristic path length (L_p) and global efficiency (E_{glob}). L_p describes how directly all pairs of nodes in the network are connected. L_p is defined as the average smallest number of connections (i.e., edges) to link all pairs of nodes. E_{glob} is inversely related to the characteristic path length and describes the capacity for parallel exchange of information within the whole network.

Modularity (Q) includes several components. Q is computed by assigning each node to a module in a participant's network so that the ratio of within-module edges to between-module edges, relative to equivalent null networks, is maximized. The resulting number of modules varies between individual graphs. However, Q does not directly reveal differences in the number of modules or their composition. Therefore, we further evaluated these components in a follow-up analysis using three indices: the total number of modules (N_{mod}), number of 'provincial hubs' (N_{prov}), and number of 'connector hubs' (N_{conn}). Provincial hubs are important for within-module communication and are identified by a high within-module degree z-score (WD) and a low participation coefficient (PC). Connector hubs are important for between-module integration and are identified by a low WD and a high PC (Cohen & D'Esposito, 2016; Guimera & Nunes, 2005; see supplement: 1.6.2).

Graph indices were calculated at each density threshold, by computing the area under the curve (AUC) for each participant at rest and during task using the function *auc()* of the R package *MESS* version 0.5.5. The AUCs were used as dependent variables (DVs) for further analyses (see section 2.7).

In addition to assessing N_{mod}, N_{prov}, and N_{conn}, we computed normalized mutual information (NMI) for each participant to explain potential differences in modular structure. NMI describes the degree of agreement between the assignment of nodes to modules in our Louvain approach and the assignment of nodes to modules/subnetworks as defined in the Power Atlas (see supplement: 1.6.3).

2.7 Statistical analyses

All statistical analyses were performed in R version 3.4.3 (R Core Team, 2017), also using the R package *afex* version 0.23–0. For all statistical tests, the level of significance was defined at 5% ($\alpha_{original} = 0.05$). Group differences in demographic, clinical, and behavioral characteristics were examined using chi-square (χ^2) tests for categorical variables and one-way analysis of variance (ANOVA) or t-tests for continuous variables. Sex was included as a factor of no interest (see supplement: 1.6) for the following analyses.

For each DV of interest (C_p, E_{loc}, Q, L_p, E_{glob}) we performed a mixed-design ANOVA (MD-ANOVA) with *group* as the between-subject factor (SZ, BD, HC) and *state* as the within-subject factor (rest, task). A strict Bonferroni-type adjustment of $\alpha_{original}$ was conducted for the five MD-ANOVAs ($\alpha_{critical} = 0.05/5 = 0.01$). To further investigate significant effects of modularity we conducted a 3×2 MD-ANOVA for each constituent variable (N_{mod}, N_{prov}, N_{conn}) with *group* as the between-subject factor and *state* as the within-subject factor. A Bonferroni-type adjustment of $\alpha_{original}$ was conducted for these follow-up MD-ANOVAs ($\alpha_{critical} = 0.05/3 = 0.016$). Post-hoc analyses were performed using t-tests and p-values were FDR adjusted. A statistical comparison of graph indices in SZ, BD subgroups (BD-I / BD-II; BD with or without a history of psychosis), and HC is included in the supplement (1.6.4, 2.4.3).

3 Results

A total of 26 participants (6 SZ, 7 BD, 13 HC) were excluded from analyses due to excessive motion or incomplete fMRI data (see supplement: 2.1). Data are presented for the final sample including 124 participants (43 SZ, 42 BD, 39 HC).

3.1 Demographic, clinical and behavioral data

Table 1 provides participant demographic, clinical, and behavioral information. The supplement (1.1) provides further information on the intake of psychiatric medications in each group. There were no differences between groups in terms of age, handedness, parental education, ethnicity, or race. The groups differed by sex and personal education. There was a lower proportion of female participants in SZ than in HC. SZ had fewer years of personal education. SZ and BD did not differ in terms of age of onset, number of hospitalizations, HAMD total, YMRS total, or mean daily doses of antipsychotic medication. SZ participants had higher BPRS and CAINS scores than BD patients. Thirty-seven out of the 42 BD patients were out of mood episode as defined by a HAMD score <15 and a YMRS score <12 (e.g., Pizzagalli, Goetz, Ostacher, Iosifescu, & Perlis, 2008). Even though no participants met criteria for a mood episode at the time of assessment, five BD patients showed mild symptoms on the HAMD (N = 4; M_{Score} = 17) or YMRS (N = 1; score = 20). There was no difference in behavioral performance on the visual perception task between groups. The average performance in each group was highly accurate, indicating ongoing vigilance and engagement with the task.

3.2 Graph analysis

Table 2 summarizes the statistical results for the main analyses on network segregation (upper panel), that is, the clustering coefficient (C_p), local efficiency (E_{loc}), and modularity (Q), and on network integration (lower panel), that is, the characteristic path length (L_p) and global efficiency (E_{glob}). Table 3 summarizes the statistical results for the follow-up analyses on three additional indices: the number of modules (N_{mod}), number of 'provincial hubs' (N_{prov}) and number of 'connector hubs' (N_{conn}). Please note, that F-, p-, and $\eta^2 G$-values for the ANOVAs are only listed in Table 1 for clarity. There was no significant *group-by-state* interaction for any of the graph indices. Both t- and p-values for post-hoc t-tests are reported in this section for significant main effects.

3.2.1   Graph indices of segregation—Fig. 2 shows the values for C_p, E_{loc}, and Q across density thresholds. Fig. 3 shows the effects of group and state on their AUC.

For C_p, there was a significant main effect of *group*, with no main effect of *state*. C_p was significantly lower in both SZ [t(118) = −3.55, $p_{FDR-corr}$ = 0.002] and BD [t(118) = −2.16, $p_{FDR-corr}$ = 0.049] compared to HC, with SZ not being significantly different from BD [t(118) = −1.49, $p_{FDR-corr}$ = 0.138]. For E_{loc}, there was a significant main effect of *state*, with no main effect of *group*. E_{loc} was higher during the task compared to rest [t(118) = 3.01, $p_{FDR-corr}$ = 0.003]. For Q, there was a significant main effect of *group*, with no main effect of *state*. Q was significantly higher in SZ compared to BD [t(118) = 2.90, $p_{FDR-corr}$ = 0.007] and HC [t(118) = 3.78, $p_{FDR-corr}$ < 0.001], both of which did not differ from each other [t(118) = 1.02, $p_{FDR-corr}$ = 0.311].

To disentangle differences in modularity, we performed follow-up analyses on three additional indices: N_{mod}, N_{prov}, and N_{conn}. Fig. 4 shows the values for N_{mod}, N_{prov} and N_{conn} across density thresholds. Fig. 5 shows a summary of the effects of group and state on their AUC.

For N_{mod}, there was a trend for a main effect of *group* and a significant main effect of *state*. N_{mod} was lower in SZ compared to HC [t(118) = −2.65, $p_{FDR-corr}$ = 0.027]. N_{mod} was higher during the task compared to rest [t(118) = 2.55, $p_{FDR-corr}$ = 0.012]. For N_{prov}, there was a significant main effect of *group* and a trend for a main effect of *state*. N_{prov} was higher in SZ compared to HC [t(118) = 3.11, $p_{FDR-corr}$ = 0.007] and BD [t(118) = 2.61, $p_{FDR-corr}$ = 0.016]. N_{prov} was lower during the task compared to rest [t(118) = −2.42, $p_{FDR-corr}$ = 0.017]. For N_{conn}, there was no significant main effect of *group* and no significant main effect of *state*.

Besides the differences in the organizational factors N_{mod}, N_{prov} and N_{conn}, there could also be group differences in the module assignment of nodes. Additional follow-up analyses did not, however, help to explain potential differences in modular structure (see supplement: 2.4.1).

In summary, the clustering coefficient (C_p) was smaller in both SZ and BD compared to HC, while modularity (Q) was higher in SZ compared to BD and HC. Local efficiency (E_{loc}) did not differ between groups, but E_{loc} was higher during task performance (relative to rest) in all groups. Thus, altered network segregation was present for both patient groups, but was more evident in SZ than in BD. Reorganization towards higher network segregation during a task compared to rest was detected to some degree across all groups and proved to be relatively normal in BD and SZ.

3.2.2   Graph indices of integration—Fig. 6 shows the values for L_p and E_{glob} across density thresholds. Fig. 7 shows the effects of group and state on their AUC.

For L_p, there was a trend for a main effect of *state*, with no main effect of *group*. L_p was lower during the task compared to rest [t(118) = −2.54, $p_{FDR-corr}$ = 0.012]. For E_{glob}, there was a trend for a main effect of *group*, with no main effect of *state*. E_{glob} was significantly higher in SZ compared to HC [t(118) = 2.85, $p_{FDR-corr}$ = 0.015], with BD not being

significantly different from either HC [t(118) = 1.83, $p_{FDR-corr}$ = 0.105] or SZ [t(118) = −1.11, $p_{FDR-corr}$ = 0.268]. However, supplemental analyses raised doubts about the stability of group differences in E_{glob} (see supplement: 2.4.2, 3.1).

In summary, network integration did not appear to be altered in patient groups, but was higher during the task state as indicated by a lower characteristic path length (L_p) compared to rest.

3.3 Exclusion of possible confounds

There was no significant main effect of *group* and no significant *group-by-state* interaction on any motion parameter. Head motion was higher during rest compared to task (see supplement: 2.2, Fig. S1), but scrubbing was performed to minimize the state differences in motion.

There were main effects of *group* and *state* on average whole-brain functional connectivity, regardless of the type of transformation used for negative correlations. Therefore, substantial effects of negative correlations on graph indices in our data were considered unlikely (see supplement: 2.3).

The pattern of results for the main graph analyses was similar using raw thresholding (see supplement: 2.4.2).

A supplemental analysis of a small subset of participants with complete coverage of 264 Power nodes revealed mostly similar means and effect sizes for the results reported in 3.2 and yielded no significant *group-by-state* interaction (see supplement: 2.4.4).

4 Discussion

The current study found group differences in functional connectome organization that were limited to network segregation, were largely state-independent, and were more evident in SZ than in BD compared to HC. Taken together, these findings provide support and refinement to theories of brain dysconnectivity in SZ and BD. In contrast, *reorganization* of the functional connectome between rest and a visual perception task was found to be relatively normal in both disorders. Thus, models of functional dysconnectivity in SZ and BD may not need to be modified to account for state-dependent changes in connectomic organization, at least based on a visual processing task.

State differences in functional network organization appeared generally consistent across clinical and healthy groups. Network segregation was higher in the task state, as reflected in higher local efficiency (E_{loc}) compared to rest. Thus, different functional brain regions appear to be more effectively compartmentalized into specialized modules when participants are performing a task. Similar to segregation, the degree of integration was higher during the task, reflected in a lower characteristic path length (L_p). This would be congruent with more direct interactions among nodes during task performance. Hence, the state differences found across groups in E_{loc} and L_p appear to reflect a broad-scale change in the functional organization of the brain related to performing a task. Although the clustering coefficient (C_p), modularity (Q), and global efficiency (E_{glob}) did not show a significant difference

between task and rest, our results on the state-dependence of the functional connectome are in line with previous findings from healthy participants and extend these by adding a comparison to patient groups (Bolt et al., 2017; Ulloa & Horwitz, 2018).

Three previous studies that found subtle differences in state-induced modulations to functional network segregation and/or integration between SZ and HC (Calhoun et al., 2006; S. Ma et al., 2012; Q. Yu et al., 2013) employed different data analytic approaches (e.g. ICA-based node definition and graph metrices averaged across a small number of thresholds versus using AUCs) and a smaller sample of patients. They also used an auditory task whereas this study used a visual task. It will be important to determine the extent to which sensory modality or task type affects the reorganization of the functional connectome in SZ using the identical data analytic approach. As these studies did not include BD, it remains to be determined whether network reorganization of BD would be modulated by sensory modality.

Anticipated group differences in functional network organization were found to the same extent across states. SZ differed from HC on one index of integration (E_{glob}). However, we are a reluctant to interpret this finding, because supplemental analyses raised doubts about its stability (see supplement: 2.4.2, 3.1). Group differences were more evident for segregation (i.e., C_p, Q). C_p was reduced in BD and SZ, consistent with previous findings (Liu et al., 2008; Lynall et al., 2010; S. Ma et al., 2012; Xia et al., 2019). This result indicates that small functional ensembles of brain regions are less internally connected in SZ and BD compared to HC. In other words, the partitioning of brain function in SZ and BD does not seem to exhibit the same degree of 'granularity' as in HC.

In SZ, Q was altered compared to HC. While both C_p and Q are global measures of segregation, they emphasize the clustering of nodes at different scales (i.e., topology of *adjacent nodes* in C_p versus 'clustering' of a *large number of nodes* in Q). Q refers to larger clusters of nodes (i.e., modules) that also include nodes which are not directly connected (i.e., not adjacent) to one another. The findings for Q suggest that individuals with BD, at least those who are out of mood episode as in the current study, maintain brain network segregation better than individuals with SZ. Because modularity is linked to cognitive performance, this view is consistent with observations that cognitive dysfunction in BD is, on average, less pronounced than in SZ (Lee et al., 2013; Lewandowski, Cohen, & Ongur, 2011).

In SZ, Q was found to be *higher* than in HC. This result is in contrast to three previous resting-state fMRI studies that showed *lower Q* in SZ. Notably, two of these studies examined a small sample of patients with childhood-onset SZ (Alexander-Bloch et al., 2010, 2012). The third study used a unique methodological approach by constructing individual functional networks at the voxel level rather than using atlas-based ROIs as nodes (Q. Ma et al., 2020). All three studies used a different algorithm to compute Q (Newman method; Newman, 2006) than the current study (Louvain method; Blondel et al., 2008). The finding of *higher Q* in SZ was also unexpected in that higher modularity is often considered better for neural processing, at least up to a certain level (Gallen & D'Esposito, 2019). However, especially for complex tasks, high modularity is often not beneficial (Cohen & D'Esposito,

2016; Park & Deem, 2012; Yue et al., 2017). Furthermore, it is possible that an *increase* in Q in psychopathology reflects sub-optimal network segregation rather than an efficient division of the brain into distinct modules.

Because Q is a multi-component measure, we performed follow-up analyses to better understand the organizational factors that contributed to higher Q in SZ. In SZ, there were more provincial hubs and fewer modules across states, resulting in greater within-module connectivity compared to HC. The lack of difference in connector hubs indicated that connectivity between a lower number of modules in SZ was similar to connectivity between a greater number of modules in HC. These findings suggest that brain function in SZ relies on larger clusters of regions that are well connected to central anchors within themselves (i.e., provincial hubs). By contrast, clusters in HC tended to be smaller but more numerous, with sparser connections converging to certain central regions. This pattern of results helps to explain why Q was higher in SZ. There were no group differences in the components of modularity between BD and HC. As in the main analyses, state differences in the follow-up analyses did not differ between groups.

The current study has several limitations. First, even though previous studies have also used scan durations of about 5 min (e.g., Lopez, Kandala, Marek, & Barch, 2020; Q. Ma et al., 2020; Martino et al., 2016), a resting-state fMRI scan of 5 min is still relatively short. On the one hand, higher reliability of functional connections and graph indices can be achieved with much longer scans (Birn et al., 2013; Gordon et al., 2017). On the other hand, a shorter scan duration reduces the risk of data contamination by confounds such as sleep and motion (Haimovici, Tagliazucchi, Balenzuela, & Laufs, 2017; Laumann et al., 2017; Meissner, Walbrin, Nordt, Koldewyn, & Weigelt, 2019; Tagliazucchi & Laufs, 2014; Vergara et al., 2019). Second, brain coverage for fMRI acquisition was not optimal given that we had to exclude about 23% of the nodes in the Power atlas. Nonetheless, follow-up analyses in a subsample with complete coverage of Power nodes showed mostly similar means and effect sizes. Third, we used only one visual task to examine task-evoked functional connectivity compared to intrinsic functional connectivity. The investigation of varying levels of task difficulty (e.g., eko et al., 2015) and different types of tasks (e.g., Bolt et al., 2017) could reveal additional rest-to-task relationships in whole-brain functional organization in BD and SZ. Fourth, our study included only individuals with chronic SZ and individuals with BD who were out of mood episode and were medicated as clinically indicated. Therefore, we do not know whether the observed differences and similarities in the organization of the functional connectome in SZ, BD, and HC might also be found in recent-onset, unmedicated, or actively symptomatic individuals. Nor can we generalize findings to BD patients who are in mood episode. Notably, past studies in BD have not identified a consistent pattern of functional connectivity changes between mood states (Brady, Margolis, Masters, Keshavan, & Öngür, 2017; Brady et al., 2016; Li et al., 2015; Syan et al., 2018; Vargas, López-Jaramillo, & Vieta, 2013).

In summary, our results indicate that although network organization is aberrant, capacity for state-dependent *reorganization* is largely intact in SZ and BD during a visual perception task. Thus, our findings add additional support to the growing consensus that functional dysconnectivity is an important feature of these disorders. At the same time, our findings

suggest that theories of dysconnectivity in SZ and BD may not need to be updated to account for illness-related alterations in network *reorganization* as a function of mental state, at least with regard to rest versus performing a visual task. Our study highlights the value of further examining state-dependent reorganization of functional networks to fully characterize network reorganization effects in these populations (e.g., with experimental manipulation of task type and difficulty level). Moreover, results need to be replicated with samples that include greater demographic and clinical variance. Nevertheless, the present findings present a useful starting point for this research by establishing that state-dependent reorganization of the functional connectome is relatively normal in SZ and BD for at least one common visual processing task.

Supplementary Material

Refer to Web version on PubMed Central for supplementary material.

Acknowledgements

References

Alexander-Bloch AF, Gogtay N, Meunier D, Birn R, Clasen L, Lalonde F, … Bullmore ET (2010). Disrupted modularity and local connectivity of brain functional networks in childhood-onset schizophrenia. Frontiers in Systems Neuroscience. 10.3389/fnsys.2010.00147

Alexander-Bloch AF, Lambiotte R, Roberts B, Giedd J, Gogtay N, & Bullmore E (2012). The discovery of population differences in network community structure: New methods and applications to brain functional networks in schizophrenia. NeuroImage, 59(4), 3889–3900. 10.1016/j.neuroimage.2011.11.035 [PubMed: 22119652]

Andreasen NC, Pressler M, Nopoulos P, Miller D, & Ho BC (2010). Antipsychotic Dose Equivalents and Dose-Years: A Standardized Method for Comparing Exposure to Different Drugs. Biological Psychiatry, 67, 255–262. 10.1016/j.biopsych.2009.08.040 [PubMed: 19897178]

Birn RM, Molloy EK, Patriat R, Parker T, Meier TB, Kirk GR, … Prabhakaran V (2013). The effect of scan length on the reliability of resting-state fMRI connectivity estimates. NeuroImage, 83, 550–558. 10.1016/j.neuroimage.2013.05.099 [PubMed: 23747458]

Blondel VD, Guillaume JL, Lambiotte R, & Lefebvre E (2008). Fast unfolding of communities in large networks. Journal of Statistical Mechanics: Theory and Experiment. 10.1088/1742-5468/2008/10/P10008

Bolt T, Nomi JS, Rubinov M, & Uddin LQ (2017). Correspondence between evoked and intrinsic functional brain network configurations. Human Brain Mapping, 38(4), 1992–2007. 10.1002/hbm.23500 [PubMed: 28052450]

Brady RO, Margolis A, Masters GA, Keshavan M, & Öngür D (2017). Bipolar mood state reflected in cortico-amygdala resting state connectivity: A cohort and longitudinal study. Journal of Affective Disorders, 217, 205–209. 10.1016/j.jad.2017.03.043 [PubMed: 28415008]

Brady RO, Masters GA, Mathew IT, Margolis A, Cohen BM, Öngür D, & Keshavan M (2016). State dependent cortico-amygdala circuit dysfunction in bipolar disorder. Journal of Affective Disorders, 201, 79–87. 10.1016/j.jad.2016.04.052 [PubMed: 27177299]

Breckel TPK, Thiel CM, Bullmore ET, Zalesky A, Patel AX, & Giessing C (2013). Long-Term Effects of Attentional Performance on Functional Brain Network Topology. PLoS ONE, 8(9), 1–14. 10.1371/journal.pone.0074125

Butler PD, Silverstein SM, & Dakin SC (2008). Visual Perception and Its Impairment in Schizophrenia. Biological Psychiatry. 10.1016/j.biopsych.2008.03.023

Calhoun VD, Adali T, Kiehl KA, Astur R, Pekar JJ, & Pearlson GD (2006). A method for multitask fMRI data fusion applied to schizophrenia. Human Brain Mapping, 27(7), 598–610. 10.1002/hbm.20204 [PubMed: 16342150]

Calhoun VD, Kiehl KA, & Pearlson GD (2008). Modulation of temporally coherent brain networks estimated using ICA at rest and during cognitive tasks. Human Brain Mapping, 29(7), 828–838. 10.1002/hbm.20581 [PubMed: 18438867]

Cao H, Dixson L, Meyer-Lindenberg A, & Tost H (2016). Functional connectivity measures as schizophrenia intermediate phenotypes: advances, limitations, and future directions. Current Opinion in Neurobiology, 36, 7–14. [PubMed: 26276700]

eko M, Gracely JL, Fitzcharles MA, Seminowicz DA, Schweinhardt P, & Bushnell MC (2015). Is a responsive default mode network required for successful working memory task performance? Journal of Neuroscience, 35(33), 11595–11605. 10.1523/JNEUROSCI.0264-15.2015 [PubMed: 26290236]

Cohen JR, & D'Esposito M (2016). The Segregation and Integration of Distinct Brain Networks and Their Relationship to Cognition. Journal of Neuroscience, 36(48), 12083–12094. 10.1523/jneurosci.2965-15.2016 [PubMed: 27903719]

Cole MW, Bassett DS, Power JD, Braver TS, & Petersen SE (2014). Intrinsic and task-evoked network architectures of the human brain. Neuron, 83(1), 238–251. 10.1016/j.neuron.2014.05.014 [PubMed: 24991964]

Doucet GE, Bassett DS, Yao N, Glahn DC, & Frangou S (2017). The role of intrinsic brain functional connectivity in vulnerability and resilience to bipolar disorder. American Journal of Psychiatry, 174(12), 1214–1222. 10.1176/appi.ajp.2017.17010095 [PubMed: 28817956]

Finc K, Bonna K, He X, Lydon-Staley DM, Kühn S, Duch W, & Bassett DS (2020). Dynamic reconfiguration of functional brain networks during working memory training. Nature Communications. 10.1038/s41467-020-15631-z

First MB, Gibbon M, Spitzer RL, Williams JB, & Benjamin LS (1997). Structured clinical interview for the DSM-IV axis I disorders (SCID-I), clinician version, user's guide. American Psychiatric Press, Inc.

Friston KJ, Brown HR, Siemerkus J, & Stephan KE (2016). The dysconnection hypothesis (2016). Schizophrenia Research, 176(2–3), 83–94. 10.1016/j.schres.2016.07.014 [PubMed: 27450778]

Friston KJ, & Frith CD (1995). Schizophrenia: a disconnection syndrome? Clin Neurosci, 3(2), 89–97. Retrieved from https://www.ncbi.nlm.nih.gov/pubmed/7583624 [PubMed: 7583624]

Fryer SL, Roach BJ, Ford JM, Donaldson KR, Calhoun VD, Pearlson GD, … Mathalon DH (2019). Should i stay or should i Go? FMRI study of response inhibition in early illness schizophrenia and risk for psychosis. Schizophrenia Bulletin. 10.1093/schbul/sbx198

Gallen CL, & D'Esposito M (2019). Brain Modularity: A Biomarker of Intervention-related Plasticity. Trends in Cognitive Sciences, 23(4), 293–304. 10.1016/j.tics.2019.01.014 [PubMed: 30827796]

Gargouri F, Kallel F, Delphine S, Hamida A. Ben, Lehéricy S, & Valabregue R (2018). The influence of preprocessing steps on graph theory measures derived from resting state fMRI. Frontiers in Computational Neuroscience. 10.3389/fncom.2018.00008

Gong J, Wang J, Chen P, Qi Z, Luo Z, Wang J, … Wang Y (2021). Large-scale network abnormality in bipolar disorder: a multimodal meta-analysis of resting-state functional and structural magnetic resonance imaging studies. Journal of Affective Disorders.

Gordon EM, Laumann TO, Gilmore AW, Newbold DJ, Greene DJ, Berg JJ, … Dosenbach NUF (2017). Precision Functional Mapping of Individual Human Brains. Neuron, 95(4), 791–807.e7. 10.1016/j.neuron.2017.07.011 [PubMed: 28757305]

Guimera R, & Nunes LA (2005). Functional cartography of complex metabolic networks. Nature, 433(7028), 859–900. 10.1038/nature03286.1.

Hadley JA, Kraguljac NV, White DM, Ver Hoef L, Tabora J, & Lahti AC (2016). Change in brain network topology as a function of treatment response in schizophrenia: A longitudinal resting-state fMRI study using graph theory. Npj Schizophrenia, 2(December 2015), 1–7. 10.1038/npjschz.2016.14 [PubMed: 28560246]

Haimovici A, Tagliazucchi E, Balenzuela P, & Laufs H (2017). On wakefulness fluctuations as a source of BOLD functional connectivity dynamics. Scientific Reports, 7(1), 5908. 10.1038/s41598-017-06389-4 [PubMed: 28724928]

Hamilton M (1960). A rating scale for depression. Journal of Neurology, Neurosurgery, and Psychiatry, 23, 56–62. 10.1136/jnnp.23.1.56 [PubMed: 14399272]

He H, Sui J, Yu Q, Turner JA, Ho BC, Sponheim SR, … Calhoun VD (2012). Altered small-world brain networks in schizophrenia patients during working memory performance. PLoS ONE, 7(6), e38195. 10.1371/journal.pone.0038195 [PubMed: 22701611]

Javitt DC, & Freedman R (2016). Sensory Processing Dysfunction in the Personal Experience and Neuronal Machinery of Schizophrenia. Am J Psychiatry. 10.1176/appi.ajp.2014.13121691.Sensory

Jenkinson M, Beckmann CF, Behrens TEJ, Woolrich MW, & Smith SM (2012). Fsl. Neuroimage, 62(2), 782–790. [PubMed: 21979382]

Jiang P, Vuontela V, Tokariev M, Lin H, Aronen ET, Ma YY, & Carlson S (2018). Functional connectivity of intrinsic cognitive networks during resting state and task performance in preadolescent children. PLoS ONE, 13(10), 1–24. 10.1371/journal.pone.0205690

Jiang T, He Y, Zang Y, & Weng X (2004). Modulation of Functional Connectivity during the Resting State and the Motor Task. Human Brain Mapping, 22(1), 63–71. 10.1002/hbm.20012 [PubMed: 15083527]

Jimenez AM, Riedel P, Lee J, Reavis EA, & Green MF (2019). Linking Resting State Networks and Social Cognition in Schizophrenia and Bipolar Disorder. Hum Brain Mapping, 40(16), 4703–4715. 10.1002/hbm.24731

Kambeitz J, Kambeitz-Ilankovic L, Cabral C, Dwyer DB, Calhoun VD, Van Den Heuvel MP, … Malchow B (2016). Aberrant Functional Whole-Brain Network Architecture in Patients with Schizophrenia: A Meta-analysis. Schizophrenia Bulletin, 42(Suppl 1), 13–21. 10.1093/schbul/sbv174

Khadka S, Meda SA, Stevens MC, Glahn DC, Calhoun VD, Sweeney JA, … Pearlson GD (2013). Is Aberrant Functional Connectivity A Psychosis Endophenotype? A Resting State Functional Magnetic Resonance Imaging Study. Biological Psychiatry, 74(6), 458–466. https://doi.org/10.1016/j.biopsych.2013.04.024 [PubMed: 23746539]

Kieliba P, Madugula S, Filippini N, Duff EP, & Makin TR (2019). Large-scale intrinsic connectivity is consistent across varying task demands. PLoS ONE, 14(4), 1–21. 10.1371/journal.pone.0213861

Kring AM, Gur RE, Blanchard JJ, Horan WP, & Reise SP (2013). The Clinical Assessment Interview for Negative Symptoms (CAINS): Final development and validation. American Journal of Psychiatry, 170(2), 165–172. 10.1176/appi.ajp.2012.12010109 [PubMed: 23377637]

Laumann TO, Snyder AZ, Mitra A, Gordon EM, Gratton C, Adeyemo B, … Petersen SE (2017). On the Stability of BOLD fMRI Correlations. Cerebral Cortex, 27(10), 4719–4732. 10.1093/cercor/bhw265 [PubMed: 27591147]

Lee J, Altshuler L, Glahn DC, Miklowitz DJ, Ochsner K, & Green MF (2013). Social and nonsocial cognition in bipolar disorder and schizophrenia: relative levels of impairment. Am J Psychiatry, 170(3), 334–341. 10.1176/appi.ajp.2012.12040490 [PubMed: 23450289]

Lei D, Pinaya WHL, van Amelsvoort T, Marcelis M, Donohoe G, Mothersill DO, … Mechelli A (2019). Detecting schizophrenia at the level of the individual: relative diagnostic value of whole-brain images, connectome-wide functional connectivity and graph-based metrics. Psychological Medicine, 1–10. 10.1017/s0033291719001934

Lewandowski KE, Cohen BM, & Ongur D (2011). Evolution of neuropsychological dysfunction during the course of schizophrenia and bipolar disorder. Psychological Medicine, 41(2), 225–241. 10.1017/S0033291710001042 [PubMed: 20836900]

Li M, Huang C, Deng W, Ma X, Han Y, Wang Q, … Li T (2015). Contrasting and convergent patterns of amygdala connectivity in mania and depression: A resting-state study. Journal of Affective Disorders, 173, 53–58. 10.1016/j.jad.2014.10.044 [PubMed: 25462396]

Liu Y, Liang M, Zhou Y, He Y, Hao Y, Song M, … Jiang T (2008). Disrupted small-world networks in schizophrenia. Brain, 131(4), 945–961. 10.1093/brain/awn018 [PubMed: 18299296]

Lopez KC, Kandala S, Marek S, & Barch DM (2020). Development of Network Topology and Functional Connectivity of the Prefrontal Cortex. Cerebral Cortex, 30(4), 2489–2505. 10.1093/cercor/bhz255 [PubMed: 31808790]

Lynall ME, Bassett DS, Kerwin R, McKenna PJ, Kitzbichler M, Muller U, & Bullmore E (2010). Functional connectivity and brain networks in schizophrenia. Journal of Neuroscience, 30(28), 9477–9487. 10.1523/JNEUROSCI.0333-10.2010 [PubMed: 20631176]

Ma Q, Tang Y, Wang F, Liao X, Jiang X, Wei S, … Xia M (2020). Transdiagnostic Dysfunctions in Brain Modules Across Patients with Schizophrenia, Bipolar Disorder, and Major Depressive Disorder: A Connectome-Based Study. Schizophrenia Bulletin, 46(3), 699–712. 10.1093/schbul/sbz111 [PubMed: 31755957]

Ma S, Calhoun VD, Eichele T, Du W, & Adali T (2012). Modulations of functional connectivity in the healthy and schizophrenia groups during task and rest. NeuroImage, 62(3), 1694–1704. 10.1016/j.neuroimage.2012.05.048 [PubMed: 22634855]

Magalhães R, Marques P, Soares J, Alves V, & Sousa N (2015). The impact of normalization and segmentation on resting-state brain networks. Brain Connectivity. 10.1089/brain.2014.0292

Martino M, Magioncalda P, Huang Z, Conio B, Piaggio N, Duncan NW, … Northoff G (2016). Contrasting variability patterns in the default mode and sensorimotor networks balance in bipolar depression and mania. Proceedings of the National Academy of Sciences of the United States of America, 113(17), 4824–4829. 10.1073/pnas.1517558113 [PubMed: 27071087]

Meissner TW, Walbrin J, Nordt M, Koldewyn K, & Weigelt S (2019). Let's take a break: Head motion during fMRI tasks is reduced in children and adults if data acquisition is distributed across sessions or days. BioRxiv, 816116. 10.1101/816116

Narr KL, & Leaver AM (2015). Connectome and schizophrenia. Current Opinion in Psychiatry, 28(3), 229–235. 10.1097/YCO.0000000000000157 [PubMed: 25768086]

Newman MEJ (2006). Modularity and community structure in networks. PNAS, 103(23), 8577–8582. [PubMed: 16723398]

Park J-M, & Deem MW (2012). Theory for the Emergence of Modularity in Complex Systems. Bulletin of the American Physical Society.

Perry A, Roberts G, Mitchell PB, & Breakspear M (2018). Connectomics of bipolar disorder: a critical review, and evidence for dynamic instabilities within interoceptive networks. Molecular Psychiatry, 1296–1318. 10.1038/s41380-018-0267-2 [PubMed: 30279458]

Pettersson-Yeo W, Allen P, Benetti S, McGuire P, & Mechelli A (2011). Dysconnectivity in schizophrenia: Where are we now? Neuroscience and Biobehavioral Reviews, 35(5), 1110–1124. 10.1016/j.neubiorev.2010.11.004 [PubMed: 21115039]

Pizzagalli DA, Goetz E, Ostacher M, Iosifescu DV, & Perlis RH (2008). Euthymic Patients with Bipolar Disorder Show Decreased Reward Learning in a Probabilistic Reward Task. Biological Psychiatry, 64(2), 162–168. 10.1016/j.biopsych.2007.12.001 [PubMed: 18242583]

Power JD, Barnes KA, Snyder AZ, Schlaggar BL, & Petersen SE (2012). Spurious but systematic correlations in functional connectivity MRI networks arise from subject motion. NeuroImage, 59(3), 2142–2154. 10.1016/j.neuroimage.2011.10.018 [PubMed: 22019881]

Power JD, Cohen AL, Nelson SM, Wig GS, Barnes KA, Church JA, … Petersen SE (2011). Functional Network Organization of the Human Brain. Neuron, 72(4), 665–678. 10.1016/j.neuron.2011.09.006 [PubMed: 22099467]

Power JD, Mitra A, Laumann TO, Snyder AZ, Schlaggar BL, & Petersen SE (2014). Methods to detect, characterize, and remove motion artifact in resting state fMRI. NeuroImage, 84, 320–341. 10.1016/j.neuroimage.2013.08.048 [PubMed: 23994314]

R Core Team. (2017). R: A language and environment for statistical computing. R Foundation for Statistical Computing, Vienna, Austria. ISBN 3-900051-07-0, URL http://www.R-project.org/. Vienna, Austria: R Foundation for Statistical Computing. Retrieved from https://www.r-project.org/

Rassovsky Y, Horan WP, Lee J, Sergi MJ, & Green MF (2011). Pathways between early visual processing and functional outcome in schizophrenia. Psychological Medicine, 41(3), 487–497. [PubMed: 20482936]

Reavis EA, Lee J, Altshuler LL, Cohen MS, Engel SA, Glahn DC, … Green MF (2020). Structural and functional connectivity of visual cortex in schizophrenia and bipolar disorder: A graph-theoretic analysis. SBO, sgaa056. https://doi.org/10.1093/schizbullopen/sgaa056 [PubMed: 33313506]

Reavis EA, Lee J, Wynn JK, Engel SA, Cohen MS, Nuechterlein KH, … Green MF (2017). Assessing neural tuning for object perception in schizophrenia and bipolar disorder with multivariate pattern analysis of fMRI data. NeuroImage: Clinical, 16(May), 491–497. 10.1016/j.nicl.2017.08.023 [PubMed: 28932681]

Reavis EA, Lee J, Wynn JK, Narr KL, Njau SN, Engel SA, & Green MF (2017). Linking optic radiation volume to visual perception in schizophrenia and bipolar disorder. Schizophrenia Research. 10.1016/j.schres.2017.03.027

Rubinov M, & Sporns O (2010). Complex network measures of brain connectivity: Uses and interpretations. NeuroImage, 52(3), 1059–1069. 10.1016/j.neuroimage.2009.10.003 [PubMed: 19819337]

Stephan KE, Friston KJ, & Frith CD (2009). Dysconnection in Schizophrenia: From abnormal synaptic plasticity to failures of self-monitoring. Schizophrenia Bulletin, 35(3), 509–527. 10.1093/schbul/sbn176 [PubMed: 19155345]

Syan SK, Smith M, Frey BN, Remtulla R, Kapczinski F, Hall GBC, & Minuzzi L (2018). Resting-state functional connectivity in individuals with bipolar disorder during clinical remission: A systematic review. Journal of Psychiatry and Neuroscience, 43(5), 298–316. 10.1503/jpn.170175 [PubMed: 30125243]

Tagliazucchi E, & Laufs H (2014). Decoding Wakefulness Levels from Typical fMRI Resting-State Data Reveals Reliable Drifts between Wakefulness and Sleep. Neuron, 82(3), 695–708. 10.1016/j.neuron.2014.03.020 [PubMed: 24811386]

Ulloa A, & Horwitz B (2018). Quantifying Differences Between Passive and Task-Evoked Intrinsic Functional Connectivity in a Large-Scale Brain Simulation. Brain Connectivity, 8(10), 637–652. 10.1089/brain.2018.0620 [PubMed: 30430844]

van de Ven V, Rotarska Jagiela A, Oertel-Knöchel V, & Linden DEJ (2017). Reduced intrinsic visual cortical connectivity is associated with impaired perceptual closure in schizophrenia. NeuroImage: Clinical. 10.1016/j.nicl.2017.04.012

Van Den Heuvel MP, & Fornito A (2014). Brain networks in schizophrenia. Neuropsychology Review, 24(1), 32–48. [PubMed: 24500505]

van Wijk BCM, Stam CJ, & Daffertshofer A (2010). Comparing brain networks of different size and connectivity density using graph theory. PLoS ONE, 5(10), e13701. 10.1371/journal.pone.0013701 [PubMed: 21060892]

Vargas C, López-Jaramillo C, & Vieta E (2013). A systematic literature review of resting state network-functional MRI in bipolar disorder. Journal of Affective Disorders, 150(3), 727–735. 10.1016/j.jad.2013.05.083 [PubMed: 23830141]

Ventura J, Nuechterlein KH, Subotnik K, & Gilbert E (1995). Symptom dimensions in recentonset schizophrenia: The 24-item expanded BPRS. Schizophrenia Research, 1(15), 22. 10.1016/0920-9964(95)95082-k

Vergara VM, Damaraju E, Turner JA, Pearlson G, Belger A, Mathalon DH, … Calhoun VD (2019). Altered Domain Functional Network Connectivity Strength and Randomness in Schizophrenia. Frontiers in Psychiatry, 10(July), 1–11. 10.3389/fpsyt.2019.00499 [PubMed: 30723425]

Wang Y, Wang J, Jia Y, Zhong S, Zhong M, Sun Y, … Huang R (2017). Topologically convergent and divergent functional connectivity patterns in unmedicated unipolar depression and bipolar disorder. Translational Psychiatry, 7(7), e1165. 10.1038/tp.2017.117 [PubMed: 28675389]

Watson CG (2018). brainGraph: Graph Theory Analysis of Brain MRI Data. Retrieved from https://github.com/cwatson/brainGraph

Xia M, Womer FY, Chang M, Zhu Y, Zhou Q, Edmiston EK, … Wang F (2019). Shared and Distinct Functional Architectures of Brain Networks Across Psychiatric Disorders. Schizophrenia Bulletin, 45(2), 450–463. 10.1093/schbul/sby046 [PubMed: 29897593]

Young RC, Biggs JT, Ziegler VE, & Meyer DA (1978). A rating scale for mania: Reliability, validity and sensitivity. British Journal of Psychiatry, 133, 429–435.

Yu Q, Sui J, Kiehl KA, Pearlson G, & Calhoun VD (2013). State-related functional integration and functional segregation brain networks in schizophrenia. Schizophrenia Research, 150(2–3), 450–458. 10.1016/j.schres.2013.09.016 [PubMed: 24094882]

Yu Q, Sui J, Rachakonda S, He H, Gruner W, Pearlson G, … Calhoun VD (2011). Altered topological properties of functional network connectivity in schizophrenia during resting state: A small-world brain Network study. PLoS ONE, 6(9), e25423. 10.1371/journal.pone.0025423 [PubMed: 21980454]

Yu Z, Qin J, Xiong X, Xu F, Wang J, Hou F, & Yang A (2020). Abnormal topology of brain functional networks in unipolar depression and bipolar disorder using optimal graph thresholding. Progress in Neuro-Psychopharmacology and Biological Psychiatry, 96, 109758. 10.1016/j.pnpbp.2019.109758 [PubMed: 31493423]

Yue Q, Martin RC, Fischer-Baum S, Ramos-Nuñez AI, Ye F, & Deem MW (2017). Brain modularity mediates the relation between task complexity and performance. Journal of Cognitive Neuroscience, 29(9), 1532–1546. 10.1162/jocn_a_01142 [PubMed: 28471728]

TASK RUNS (5)

~ 200 s

OBJECT STIMULUS BLOCKS (10 + 2)

+   +

~ 14 s

VISUAL STIMULUS PRESENTATIONS (10)

+

FLASH ON

FLASH OFF

BUTTON PRESS

1 s

400 ms

...

Figure 1.
Visual object-perception task.

Graph Indices of Network Segregation
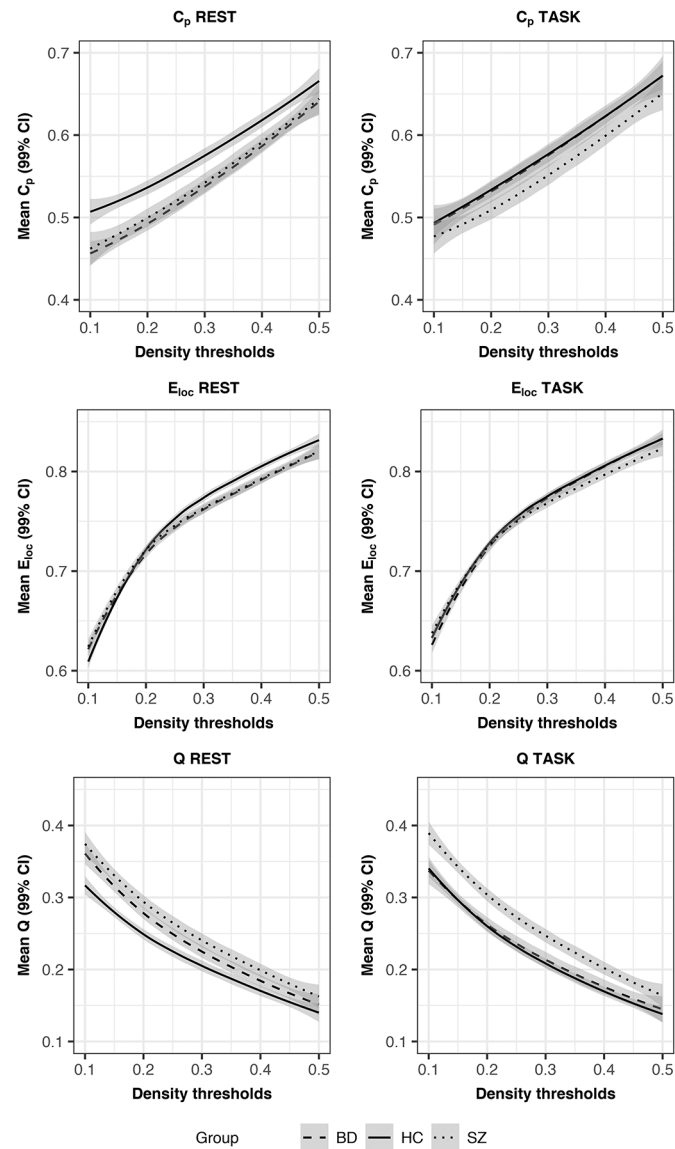
Group Means across Thresholds for REST and TASK

Figure 2.
Group means and 99% confidence intervals (CI; according to $\alpha_{\text{critical}} = 0.01$ for MD-ANOVAs) for each graph index of segregation across density thresholds for rest and task. Clustering coefficient (C_p), Local efficiency (E_{loc}), Modularity (Q).

Graph Indices of Network Segregation
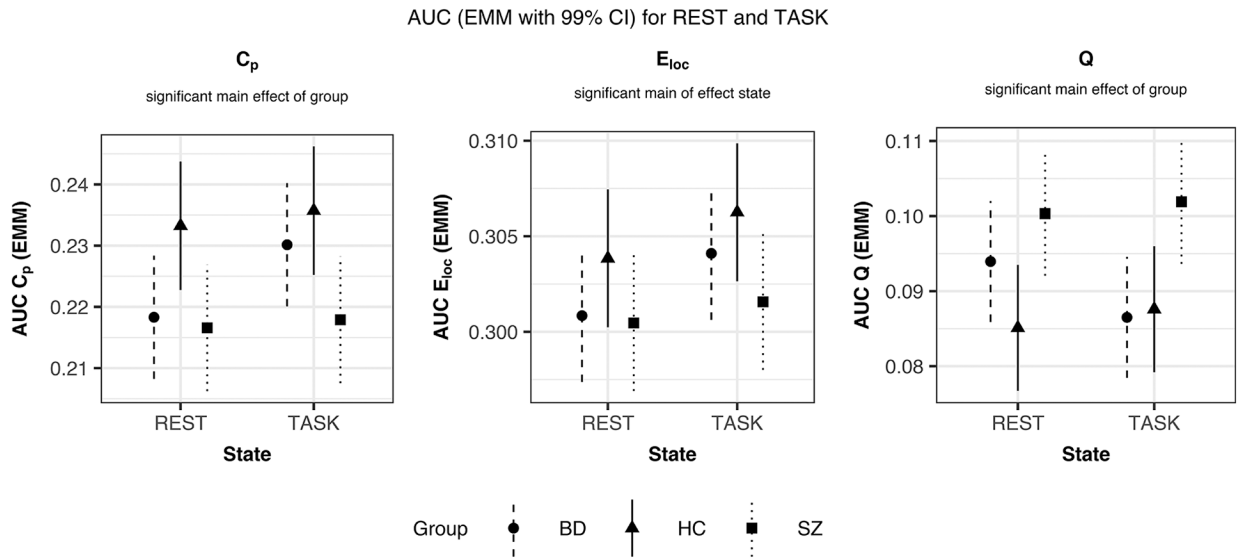
AUC (EMM with 99% CI) for REST and TASK

Figure 3.
Estimated marginal means (EMM) and 99% confidence interval (CI; according to $\alpha_{critical}$ = 0.01 for MD-ANOVAs) for the AUC of each graph index of network segregation across groups and state. Clustering coefficient (C_p), Local efficiency (E_{loc}), Modularity (Q).

Components of Modularity

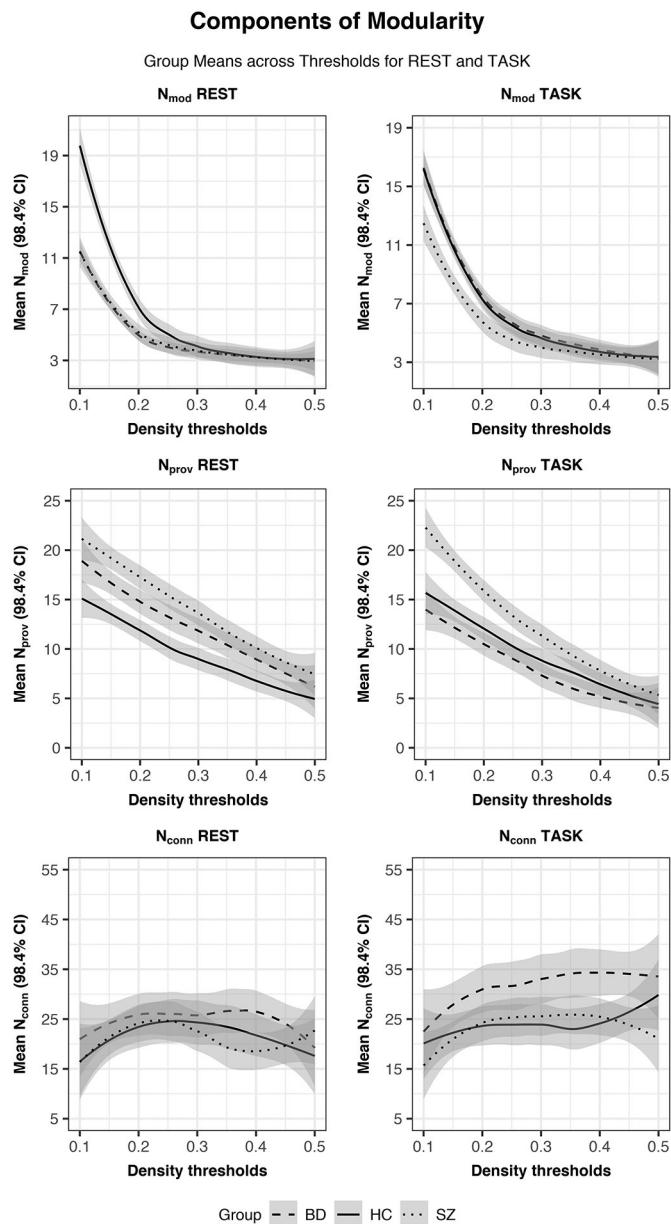Group Means across Thresholds for REST and TASK

Figure 4.
Group means and 98.4% confidence intervals (CI; according to $\alpha_{critical} = 0.016$ for explanatory MD-ANOVAs) for each component of modularity across density thresholds for rest and task. Number of modules (N_{mod}), number of 'provincial hubs' (N_{prov}), number of 'connector hubs' (N_{conn}).

Components of Modularity

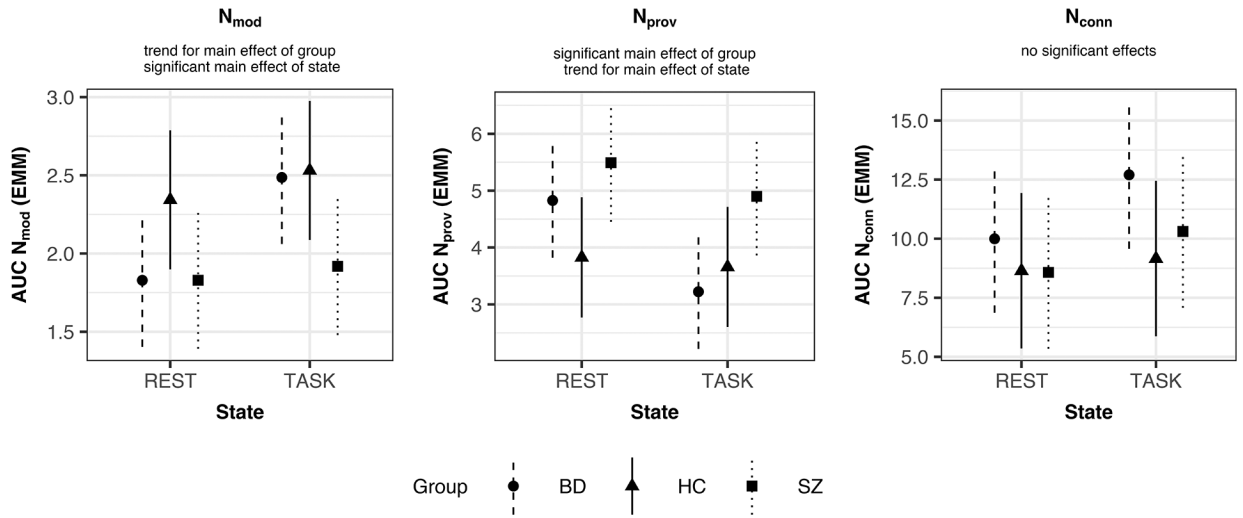AUC (EMM with 98.4% CI) for REST and TASK

Figure 5.

Estimated marginal means (EMM) and 98.4% confidence interval (CI; according to $\alpha_{critical}$ = 0.016 for explanatory MD-ANOVAs) for the AUC of each component of modularity across groups and state. Number of modules (N_{mod}), number of 'provincial hubs' (N_{prov}), number of 'connector hubs' (N_{conn}).

Graph Indices of Network Integration

Group Means across Thresholds for REST and TASK

Figure 6.
Group means and 99 % confidence intervals (CI; according to $\alpha_{critical} = 0.01$ for MD-ANOVAs) for each graph index of network integration across density thresholds for rest and task. Characteristic path length (L_p), Global efficiency (E_{glob}).

Graph Indices of Network Integration

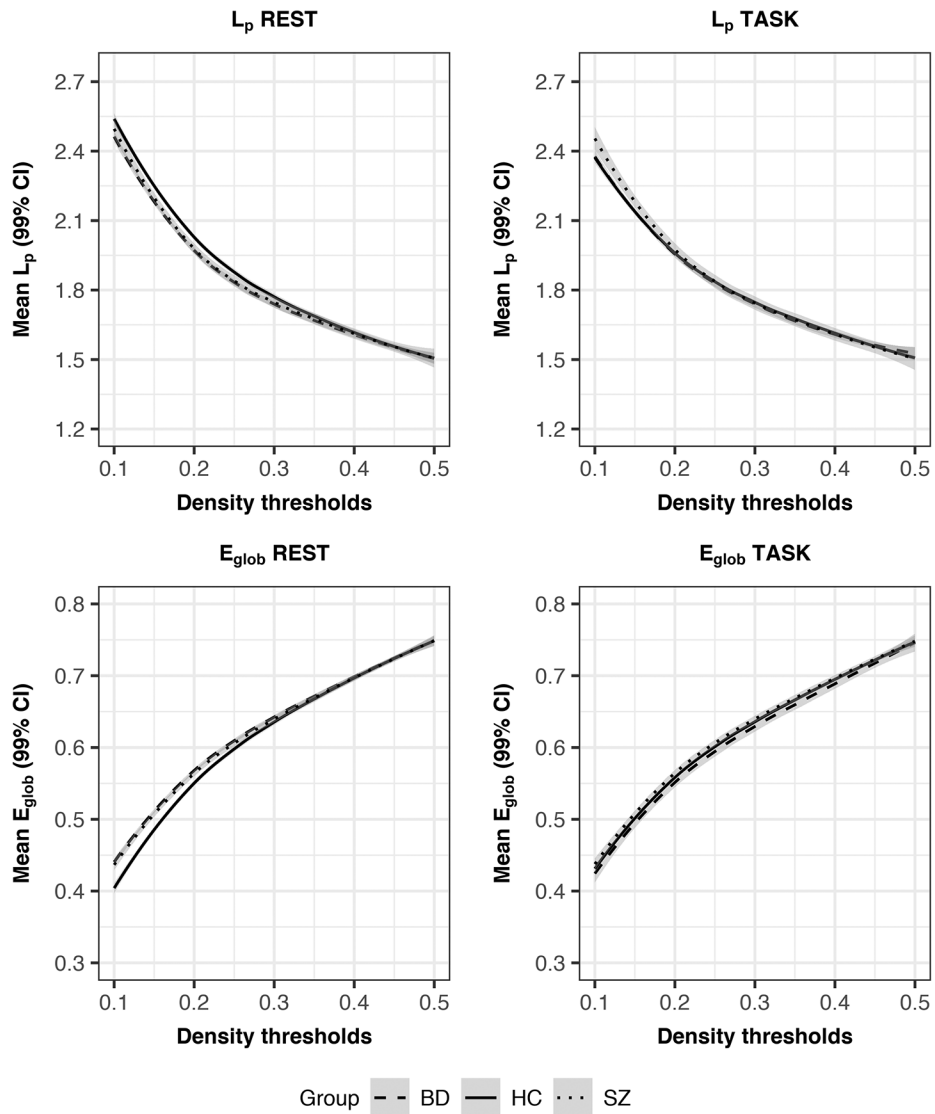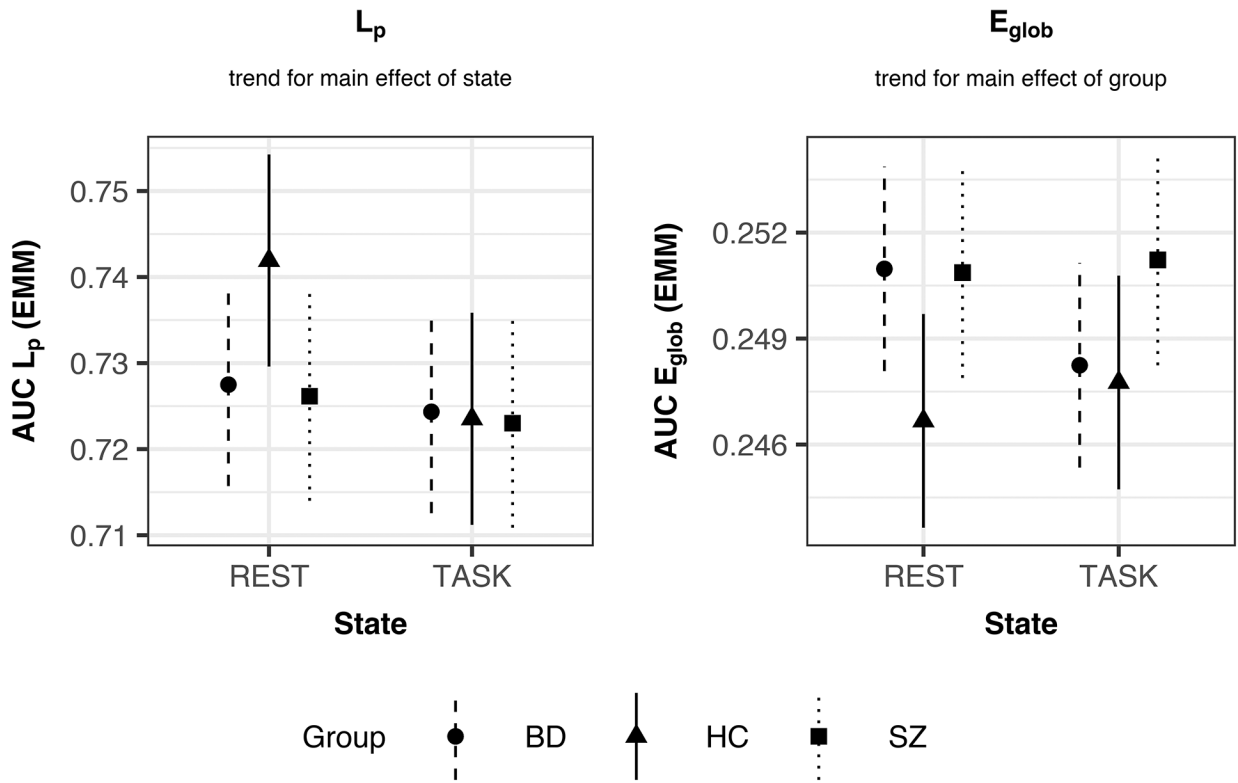## AUC (EMM with 99% CI) for REST and TASK

Figure 7.
Estimated marginal means (EMM) and 99% confidence interval (CI; according to $\alpha_{critical}$ = 0.01 for MD-ANOVAs) for the AUC of each graph index of network integration across groups and state. Characteristic path length (L_p), Global efficiency (E_{glob}).

Table 1.

Demographic, clinical and behavioural data.

Characteristic	SCZ (N = 43)	BD (N = 42)	HC (N = 39)	Group Comparison
Sex	29M 14F	20M 22F	14M 25F	$\chi^2(2) = 8.4$, **p = 0.02** [*]
Handedness	36R 7L	37R 4L	35R 4L	$\chi^2(2) = 1.0$, p = 0.60
Ethnicity	25.6	23.8	18.0	$\chi^2(2) = 0.74$, p = 0.69
% Hispanic				
Race				
% Caucasian	62.8	69.0	46.1	$\chi^2(6) = 8.1$, p = 0.23
% African American	20.9	11.9	30.8	
% Asian	4.7	2.4	10.3	
% other	11.6	16.7	12.8	
	Mean (SD)	Mean (SD)	Mean (SD)	
Age	46.09 (11.9)	43.43 (13.0)	46.39 (8.3)	$F(2,121) = 0.9$, p = 0.43
Yr. Personal Education	13.07 (2.14)	14.24 (2.38)	14.23 (1.88)	$F(2,120) = 4.1$, **p = 0.02** [*]
Yr. Parental Education	12.85 (2.89)	14.19 (2.62)	13.75 (2.39)	$F(2,113) = 2.6$, p = 0.08
Age of Onset	22.07 (7.34)	20.77 (9.38)		$t(80) = 0.7$, p = 0.49
No. Hospitalizations	6.98 (6.59)	5.28 (7.79)		$t(77) = 1.1$, p = 0.30
CPZ equivalent[a]	424.56 (342.06)	298.27 (176.80)		$t(51) = 1.6$, p = 0.13
BPRS Total	39.40 (10.36)	33.00 (5.33)		$t(82) = 3.5$, **p < 0.001** [*]
CAINS Motivation	1.63 (0.73)	1.00 (0.73)		$t(83) = 4.0$, **p < 0.001** [*]
CAINS Expressive	1.21 (0.86)	0.52 (0.71)		$t(83) = 4.0$, **p < 0.001** [*]
YMRS Total	4.56 (3.78)	3.17 (4.09)		$t(83) = 1.6$, p = 0.11
HAMD (21-item Total)	6.02 (4.94)	6.31 (4.69)		$t(83) = -0.3$, p = 0.79
Visual Perception Task				
% correct responses	99.07 (0.41)	98.71 (1.67)	99.01 (0.20)	$F(2,120) = 1.5$, p = 0.22

Abbreviations: BD, bipolar disorder; BPRS, Brief Psychiatric Rating Scale; CAINS, Clinical Assessment Interview for Negative Symptoms; CPZ equivalent, chlorpromazine equivalent; F, female; HAMD, Hamilton Depression Rating Scale; HC, healthy controls; L, left; M, male; R, right; SZ, schizophrenia; SD, standard deviation; YMRS, Young Mania Rating Scale.

[*] significant

[a] We could confirm that thirty-two participants in the SZ and twenty-one participants in the BD group were prescribed an antipsychotic medication. Mean chlorpromazine (CPZ) equivalent doses for each group were computed based on these participants. For more information on the intake of psychiatric medications, please refer to the supplement (1.1).

Table 2.

Main and interaction effects of MD-ANOVAs for graph indices of segregation (top) and integration (bottom).

MAIN GRAPH ANALYSES				
SEGREGATION				
Graph Index	**ANOVA**			**Post-hoc t-test** (α = 0.05, FDR-corr.)
	F	**p** ($\alpha_{critical}$ = 0.01)	$\eta^2{}_G$	
Cp				
Group	6.35	**0.002**[*]	**0.070**	**HC > BD**[*] **HC > SZ**[*]
State	4.43	0.037	0.010	
Group-by-State	1.9	0.154	0.008	
Eloc				
Group	2.7	0.070	0.030	**Task > Rest**[*]
State	9.04	**0.003**[*]	**0.020**	
Group-by-State	0.7	0.491	0.002	
Q				
Group	7.8	**< 0.001**[*]	**0.090**	**SZ > HC**[*] **SZ > BD**[*]
State	0.3	0.569	0.001	
Group-by-State	2.7	0.071	0.010	
INTEGRATION				
Graph Index	**ANOVA**			**Post-hoc t-test** (α = 0.05, FDR-corr.)
	F	**p** ($\alpha_{critical}$ = 0.01)	$\eta^2{}_G$	
Lp				
Group	1.3	0.277	0.010	**Task < Rest**[*]
State	6.45	**0.012**[†]	**0.020**	
Group-by-State	2.38	0.097	0.010	
Eglob				
Group	4.2	**0.018**[†]	**0.040**	**SZ > HC**[*]
State	0.3	0.585	0.001	
Group-by-State	2.3	0.104	0.010	

Significant [*] and trend-level [†] results after Bonferroni type correction of $\alpha_{original}$ are highlighted in grey.

Clustering coefficient (C_p), Local efficiency (E_{loc}), Modularity (Q), Characteristic path length (L_p), Global efficiency (E_{glob}). η^2G = generalized eta-squared.

Table 3.

Main and interaction effects of follow-up MD-ANOVAs for components of modularity.

FOLLOW-UP ANALYSES FOR COMPONENTS OF MODULARITY			
Component of modularity	**ANOVA**		**Direction of differences**
	F	**p** $(\alpha_{critical} = 0.016)$	
N mod			
Group	3.5	**0.033** [†]	**SZ < HC** **Task > Rest**
State	6.5	**0.012** [*]	
Group-by-State	2.2	0.119	
N prov			
Group	5.6	**0.005** [*]	**SZ >HC** **SZ > BD** **Task < Rest**
State	5.9	**0.017** [†]	
Group-by-State	0.3	0.607	
N conn			
Group	1.8	0.178	
State	2.5	0.114	
Group-by-State	0.4	0.689	

Significant [*] and trend-level [†] results after Bonferroni type correction of $\alpha_{original}$ are highlighted in grey.

Number of modules (N_{mod}), number of 'provincial hubs' (N_{prov}), number of 'connector hubs' (N_{conn}).